

# DISTINGUISHING CAUSAL SEEDS FROM INFLATION

Wayne Hu,<sup>1</sup> David N. Spergel<sup>2,3</sup> & Martin White<sup>4</sup>

<sup>1</sup>*Institute for Advanced Study, School of Natural Sciences  
Princeton, NJ 08540*

<sup>2</sup>*Princeton University Observatory  
Princeton, NJ 08544*

<sup>3</sup>*Department of Astronomy, University of Maryland  
College Park, MD 20742*

<sup>4</sup>*Enrico Fermi Institute, University of Chicago  
Chicago, IL 60637*

Causal seed models, such as cosmological defects, generically predict a distinctly different structure to the CMB power spectrum than inflation, due to the behavior of the perturbations outside the horizon. We provide a general analysis of their causal generation from isocurvature initial conditions by analyzing the role of stress perturbations and conservation laws in the causal evolution. Causal stress perturbations tend to generate an isocurvature pattern of peak heights in the CMB spectrum and shift the first compression, i.e. main peak, to smaller angular scales than in the inflationary case, unless the pressure and anisotropic stress fluctuations balance in such a way as to reverse the sense of gravitational interactions while also maintaining constant gravitational potentials. Aside from this case, these causal seed models can be cleanly distinguished from inflation by CMB experiments currently underway.

## Contents

<b>I</b>	<b>Introduction</b>	<b>2</b>
<b>II</b>	<b>Conservation Laws and Stress Perturbations</b>	<b>2</b>
	A Non-relativistic Example . . . . .	2
	B Relativistic Generalization . . . . .	3
	C Scaling Stress Sources . . . . .	5
<b>III</b>	<b>Implications for the CMB</b>	<b>6</b>
	A Acoustic Sources and Signatures . . . . .	6
	B Scaling Ansatz for Pressure . . . . .	7
	C Scaling Ansatz for Anisotropic Stress . . . . .	9
	D Underlying Assumptions . . . . .	10
<b>IV</b>	<b>Discussion</b>	<b>11</b>
	<b>APPENDIXES</b>	<b>13</b>
<b>A</b>	<b>Relativistic Perturbation Theory with Seeds</b>	<b>13</b>
	1 Gauge Transformations . . . . .	13
	2 Synchronous Gauge . . . . .	14
	3 Newtonian Gauge . . . . .	15
	4 Comoving Gauge . . . . .	16
<b>B</b>	<b>Causal Constraints</b>	<b>16</b>
	1 Initial Conditions . . . . .	17
	2 Stress Structure . . . . .	18
<b>C</b>	<b>Mimicking Inflation</b>	<b>19</b>

## I. INTRODUCTION

It is now widely recognized that features in the power spectrum of Cosmic Microwave Background (CMB) anisotropies can be a gold mine of information for cosmology. A great deal of experimental effort is being expended in order to map the CMB accurately over a wide range of angular scales from the ground, balloons and eventually space. In addition to providing valuable information about the cosmological parameters, it is becoming clear that the CMB can teach us much about how the fluctuations were generated in the early universe. For example in [1], it was claimed that by studying the acoustic signature of the anisotropy spectrum one can test the inflationary paradigm for fluctuation generation (see [2] and references therein for other inflationary tests).

The key idea in differentiating inflation from other models of structure formation, such as defects [3–5], is the behavior of the gravitational potential fluctuations outside the horizon. In inflation, these potentials are approximately constant while in a viable defect model, or indeed any isocurvature model, they start out vanishingly small and are generated as a mode enters the horizon. Coupled with the effects of photon backreaction, this distinction implies a different structure in the anisotropy spectrum on small angular scales, allowing for a test of the inflationary paradigm. Specifically it was claimed that, with some exotic exceptions, isocurvature models produced spectra whose peaks were phase shifted with respect to the inflationary models [1]. In a very rough sense, the inflationary driving force excites a cosine mode whereas the isocurvature one excites a sine mode. Even if the phase shift were closer to  $\pi$  rather than  $\pi/2$  radians [4], causing the peaks to line up with the inflationary model once again, the non-monotonic modulation of the peak heights by baryon drag would allow the defect and inflationary spectra to be distinguished. We refer the reader to [1] for more details.

In this paper, we specialize the discussion to causal *scaling* models by applying Turok’s [6] mode expansion techniques to the underlying stress perturbations. These fluctuations are the fundamental source of gravitational instability in any isocurvature model [7,8]. Detailed discussions of stress perturbations, conservation laws, and gauge in relativistic perturbation theory as well as their role in causality arguments are given in the Appendices A and B respectively. We explicitly enforce energy-momentum conservation and thus self-consistently include the response and backreaction of the photon-baryon fluid to the gravitational sources [1]. We show that except for one special case, the resultant CMB spectra are easily distinguished from their inflationary counterpart. If the dynamical effects of isotropic and anisotropic stress are exactly balanced, a novel situation may arise in which the sense of gravity is reversed and hence also the predictions for the acoustic features in the CMB. We discuss in detail the model of Turok [9] which utilizes this mechanism in Appendix C. Thus out of the general class of causal models with scaling properties only this one case may be confused with inflation from its acoustic signature.

## II. CONSERVATION LAWS AND STRESS PERTURBATIONS

Let us assume that the fluctuations which eventually form large scale structure in the universe are generated causally from an initially homogeneous and isotropic Friedman-Robertson-Walker universe. Causality, together with energy and momentum conservation, places strong constraints on the manner in which this can occur. Heuristically, energy conservation implies that changes in the energy density at any location arise only by its “flow” across surfaces. In general, these flows must obey momentum conservation and hence only arise from stress variations in the matter, e.g. for a perfect fluid from gradients in the pressure. It is instructive first to consider the simple case of a non-relativistic fluid. We shall then show how these arguments manifest themselves in relativistic perturbation theory with a more general stress-energy tensor for the matter.

### A. Non-relativistic Example

Here we first examine the evolution of perturbations in a simple non-relativistic fluid, perhaps with viscosity, but ignoring gravitational effects. Energy-momentum conservation for the perturbations is described by the linearized continuity and Euler fluid equations

$$\begin{aligned}\dot{\delta} &= -\partial_i v_i, \\ \rho \dot{v}_i &= \partial_i p - \partial_j \Pi_{ij},\end{aligned}\tag{1}$$

where summation is implicit,  $\delta = \delta\rho/\rho$  is the density fluctuation,  $v_i$  is the bulk velocity,  $p$  is the pressure, and  $\Pi_{ij}$  is the viscous or anisotropic stress tensor. Density fluctuations can only be generated by fluid flows. A Fourier

decomposition of the perturbation implies that compared with velocities, the density must be suppressed by a factor of  $k$  at long wavelengths. However momentum conservation constrains the form of such flows: they cannot be present initially and thus must be generated by pressure gradients. The Fourier decomposition shows that velocities should be suppressed with respect to pressure fluctuations by a factor of  $k$  at long wavelengths. Hence density fluctuations generically scale as  $k^2$  times the pressure fluctuations in a fluid or  $k^4$  in the power spectrum. This is the familiar result that causal flows of matter will establish a  $k^4$  density spectrum even when no density perturbations exist initially [11–14].

The Poisson equation implies that the resultant potential fluctuations scale as the pressure itself. In a relativistic context, potential fluctuations are equivalent to curvature fluctuations in the spatial metric. The fact that the generator of density and curvature fluctuations is causal requires that initially they must vanish. Hence we refer to such models for fluctuation generation as *isocurvature* models.

The form of the pressure perturbation itself is not arbitrary. In fact, if the pressure perturbations are adiabatic  $\delta p = (\dot{p}/\dot{\rho})\delta\rho \equiv c_s^2\delta\rho$ , then energy-momentum conservation requires  $\delta\rho = 0$  and fixes  $\delta p = 0$ , so that it cannot generate density perturbations. Thus it is only the non-adiabatic pressure or “entropy” perturbation that can causally produce density fluctuations [7]

$$p\Gamma = \delta p - c_s^2\delta\rho. \quad (2)$$

In general, there are many possible sources of non-adiabatic pressure, but causality constrains their behavior by requiring that their fluctuations be uncorrelated outside the horizon. One natural way to obtain them is to assume the fluid is composed of a sum over  $i$  particle constituents. In this case,

$$p\Gamma = \sum_i [p_i\Gamma_i + (c_i^2 - c_s^2)\delta\rho_i], \quad (3)$$

so that if the sound speed  $c_i$  in the components does not equal the total sound speed, i.e. the equation of state for the components differ, then the initial condition  $\delta\rho = \sum_i \delta\rho_i = 0$  implies that non-adiabatic pressure perturbations *must* be generated. In the cosmological setting, concrete examples of this mechanism include the baryon and axion isocurvature models as well as cosmological defect scenarios. This idea, that density fluctuations may be balanced to satisfy total energy-momentum conservation, is conventionally referred to as *compensation*. Compensation once established initially is maintained by energy-momentum conservation; there is no need to enforce it by hand as often done in the literature [4].

Now let us consider the anisotropic stress. Internal friction or viscosity is generated when there is relative motion between various parts of the fluid. The anisotropic stress tensor thus scales as the spatial derivatives of the velocity field and to lowest order, the first derivative (see e.g. [15]). By momentum conservation, we know that the velocity field vanishes initially. Hence anisotropic stress is only generated after pressure gradients set up bulk motion. The scaling in  $k$ -space is that of  $k$  times the velocity fluctuation or  $k^2$  times the pressure fluctuations. The Euler equation thus implies that *at large scales* the generation of bulk velocities and hence density and potential fluctuations through anisotropic stress is subdominant.

This simple example shows that the energy-momentum conservation equations automatically build in causal behavior. The problem of considering the effects of causality thus reduces to the establishment of causal initial conditions and the enforcement of energy-momentum conservation as the universe evolves under the stresses of the matter.

## B. Relativistic Generalization

Two issues complicate the simple picture of the last section. The first is that we must possess a model for how the stress perturbations evolve. We shall return to consider causal constraints on their behavior in the next section. The second is that in relativistic perturbation theory, the stress-energy tensor of the matter is *covariantly* conserved. Hence the continuity and Euler relations of Eq. (1) become

$$T^{0\nu}{}_{;\nu} = 0, \quad T^{i\nu}{}_{;\nu} = 0. \quad (4)$$

Because metric terms enter these equations, the form that the causal constraint takes depends on the metric representation, i.e. the gauge. For example, the continuity equation is altered by changes in the spatial metric. The simplest example is that of the stretching of space due to the background expansion, which dilutes the number density of particles in physical space. Likewise perturbations to the spatial metric cause similar effects to the density perturbation. To disentangle metric effects on the generation of perturbations from the truly causal evolution by flows, it

is desirable to find a representation of perturbations that obeys an ordinary conservation law. In this context, two quantities have been often discussed in the literature: the stress-energy pseudo-tensor  $\tau_{\mu\nu}$  [16,17] and the comoving curvature perturbation  $\zeta$  [7,18].

To understand the problem, it is perhaps useful to recall first the issue of gauge choice. In relativistic perturbation theory, one has the freedom to choose which spatial surface, and what coordinate system on this surface, to use in defining the perturbations. Gauge freedom can be both a complicating annoyance and a very convenient tool, but poses no real obstacle for applying relativistic perturbation theory. Once the initial conditions are properly established, covariant conservation of the stress-energy tensor properly and causally evolves the fluctuations in any gauge. In particular, all gauges will agree on *physical observables*, e.g. CMB anisotropies. Three gauge choices, for which we give detailed properties in Appendix A, are in common use. Let us briefly note here their benefits and drawbacks before specializing the discussion to the relativistic analogue of the initial conditions described in the previous section.

Perhaps the most popular gauge choice is that of synchronous gauge, where the perturbations appear only in the space-space part of the metric (see e.g. [19]). In this gauge, the spatial hypersurfaces on which one defines the perturbations are orthogonal to constant-time hypersurfaces and proper time corresponds to coordinate time. Thus this coordinate system is natural for freely-falling observers or cold dark matter particles. The drawback of this gauge is that the density perturbations are not easily related to the observable anisotropy and the gravitational sector is non-intuitive. One must be careful to compute observables as the individual components of this gauge can be quite misleading.

The most familiar gauge from courses in relativity is the conformal Newtonian gauge. In this gauge, the metric is diagonal: the space-space part gives the curvature perturbation, and the time-time part the gravitational potential. This gauge has been frequently used in analytic work on CMB anisotropies because the representation of the gravitational (Sachs-Wolfe) effects is simple and the density perturbations correspond closely to the CMB anisotropy. The gauge can be difficult to work with numerically, and extreme care must be taken with the initial conditions.

For work involving causality, the obvious gauge choice is the comoving gauge, also known as the total-matter gauge and velocity-orthogonal isotropic gauge. This gauge is difficult to conceptualize, since it contains an off-diagonal time-space perturbation. However as we shall show in Appendix B, the spurious effects of density dilution (from stretching of the spatial metric) which complicate the analysis of the conservation laws are absent in this gauge. More specifically, the curvature perturbation  $\zeta$  in this gauge (superscript  $T$ ) is generated only by pressure (non-adiabatic if the curvature vanishes initially) and anisotropic stress fluctuations  $\pi$  (see Eq. (A24), definitions in §A 4, and [20] for anisotropic stress terms in the relativistic fluid context)

$$\dot{\zeta} = -\frac{\dot{a}}{a} \frac{1}{\rho + p} (\delta p^T - \frac{2}{3} \pi), \quad (5)$$

where  $a$  is the scale factor and temporal derivatives are hereafter with respect to conformal time  $\tau = \int dt/a$ . In the case of a more general stress-energy tensor, we can merely replace  $\delta p$  and  $\pi$  by the isotropic and anisotropic scalar components of  $T_j^i$  [see Eq. (A4)].

The direct dependence of the curvature on stress perturbations implies that the causality argument in this gauge is the most similar to the non-relativistic case discussed in the previous section. For example, in the absence of these stresses, e.g. in the inflationary example with adiabatic fluctuations, the curvature is simply constant outside the horizon to leading order [21,22]. Thus the proper generalization of the causal argument to the relativistic context is that the curvature on the comoving hypersurfaces  $\zeta$  vanishes initially and is only generated by the causal motion of matter (see [1,7] and Appendix B).

From this condition, it is simple to reconstruct the causal constraint in the two other gauges from gauge transformations (see §B 1). The curvature on Newtonian hypersurfaces is directly proportional to the density fluctuations on the comoving hypersurfaces [see Eq. (B7)]. This suggests that the isocurvature condition for the total matter gauge is the same as that of the Newtonian gauge. We show in Appendix B that this intuition is correct, up to an irrelevant decaying mode [see Eq. (B9)], if the equation of state is constant. For the synchronous gauge, the condition that  $\zeta = 0$  is identical to the assumption that the pseudo-energy  $\tau_{00}$  and the pseudo-momentum density  $\tau_{0i}$  defined in Eq. (B5) vanishes initially [16]. These are components of the stress-energy pseudo-tensor commonly employed in the literature, which likewise obeys an ordinary conservation condition

$$\dot{\tau}_{00} = \partial^i \tau_{0i}, \quad (6)$$

as one would expect. Thus these three sets of initial conditions: vanishing of the comoving curvature  $\zeta$ , Newtonian curvature  $\Phi$ , and  $\tau_{00}$ ,  $\tau_{0i}$ , are essentially equivalent. Once these conditions are established, energy-momentum conservation causally evolves the perturbations under the influence of spatial stresses, generating properties such as a

$k^4$  scaling in the power spectrum of the pseudo-energy and comoving density perturbation. Let us now turn to the question of causal stress evolution.

### C. Scaling Stress Sources

Causality implies that no measurable quantity, e.g. the fields and stress-energy components, can have superhorizon scale correlations. This implies that their power spectrum behaves as “white noise”,  $k^0$  to leading order for  $k\tau \ll 1$ , unless other symmetries exist to eliminate even this contribution (e.g. energy-momentum conservation and the comoving density perturbation, see also §B2). In Appendix B, we show that for models with scalar fields, this constraint limits the superhorizon scale behavior of all of the stresses: the isotropic stress  $p_s$  behaves as  $k^0$  and the anisotropic stresses, which depend only on spatial derivatives of fields, behaves as  $k^2$  for  $k\tau \ll 1$ .

Turok [6] raises the interesting question of what general statements for the CMB anisotropy spectrum can be made if one combines causality with the *scaling ansatz*. The scaling ansatz is a powerful tool for analyzing the dynamics and predictions of defect models [23–25]. It implies that defect networks have only one characteristic scale, set by the current horizon size. Thus, for example, a string network a few thousand years after the big bang has the same correlations as a string network a nanosecond after the big bang. This scaling ansatz has been useful for studying the dynamics of the non-linear sigma model, a simple approximation to defect dynamics, that has scaling solutions in both the matter and radiation dominated epochs [26,27].

For our purposes, scaling may be defined more phenomenologically as the assumption that the power (per  $\log k$ ) in the metric fluctuations, i.e. in the Newtonian curvature fluctuation  $k^3|\Phi|^2$ , and potential fluctuation  $k^3|\Psi|^2$  are both the same on each scale at horizon crossing  $k\tau = 1$  and evolve in a self-similar fashion

$$\Phi = k^{-3/2}f(k\tau), \quad \Psi = k^{-3/2}g(k\tau). \quad (7)$$

The Newtonian potential and curvature perturbations along with their evolution are directly related to the gravitational redshifts experienced by a photon [28]. Thus *any* model which can explain the flatness of the large angle CMB spectrum seen by *COBE* [29] must also obey the scaling ansatz at least approximately. The inflationary scenario naturally generates such fluctuations with  $f(k\tau) = g(k\tau) = \text{constant}$ . We must now seek a causal mechanism for their generation through stress perturbations. The ansatz cannot simply be imposed on the metric fluctuations since this does not guarantee that a consistent solution of the conservation and Einstein-Poisson equations exist.

Consider first the Newtonian curvature  $\Phi$ . From the arguments of §II A & §II B, made rigorous by the gauge considerations of the Appendices A and B, a pressure fluctuation source  $p_s$  generates a comoving gauge density perturbation (superscript  $T$ ) of order

$$\rho\delta^T \sim (k\tau)^2 p_s, \quad (8)$$

and hence from the Newtonian Poisson equation (B7)

$$\begin{aligned} k^2\Phi &\sim 4\pi G a^2 \rho\delta^T \\ &\sim 4\pi G (a^2 p_s)(k\tau)^2. \end{aligned} \quad (9)$$

For white noise pressure perturbations, the scaling ansatz Eq. (7) then requires

$$a^2 p_s \propto \tau^{-1/2}, \quad (10)$$

for  $k\tau \ll 1$ . Thus if we adopt this ansatz for the pressure source, energy-momentum conservation will naturally generate scaling behavior in  $\Phi$ . Note also that white noise pressure perturbations imply white noise curvature fluctuations.

Turok [6] points out that to study possible behaviors around and after horizon crossing, we can decompose the source into basis functions that satisfy scaling and a strict lack of correlations outside the horizon

$$\langle a^2 p_s(k, \tau) a'^2 p_s(k', \tau') \rangle = \tau^{-1/2} \tau'^{-1/2} \sum_A \sum_{A'} P_{AA'} f_A(k\tau) f_{A'}(k'\tau'), \quad (11)$$

for which in real space

$$\langle f_A(r, \tau) f_{A'}(0, \tau') \rangle = 0 \quad \text{for} \quad r > \tau + \tau'. \quad (12)$$

The symmetry in  $k\tau$  implies that a diagonal basis exists where  $P_{AA'} = \delta_{AA'} P_A$  [6]. However, for illustrative purposes, we follow Turok in employing

$$f_A \equiv \frac{\sin(Ak\tau)}{(Ak\tau)}, \quad (13)$$

as a convenient basis, where  $0 < A < 1$ . We shall therefore adopt in the next section pressure sources of the form  $a^2 p_s \propto \tau^{-1/2} f_A$  which differs from Turok's suggestion of  $a^2(\rho_s + 3p_s) \propto \tau^{-1/2} f_A$  (see also Appendix C). Our assumption follows from scaling and causal constraints on stresses and allows the density evolution to be naturally determined by energy-momentum conservation from the source stresses.

Now let us consider the Newtonian gravitational potential [see Eq. (A18)],

$$\Psi = -\Phi - 8\pi G a^2 \pi_s / k^2. \quad (14)$$

Thus the scaling ansatz for  $\Phi$  holds equally well for  $\Psi$  except in the presence of anisotropic stress contributions  $\pi_s$ . To produce a flat CMB anisotropy spectrum, any such contributions must also obey a scaling relation

$$a^2 \pi_s \propto \tau^{-1/2} f_B(k\tau). \quad (15)$$

If the universe is isotropic initially, anisotropic stress like the comoving density perturbation can only be generated by causal motion of matter implying a  $k^2$  scaling for  $k\tau \ll 1$  (see §II A for an example). The same arguments employed in deriving the general form of the causal pressure source imply (see [9] for an analogous derivation)

$$f_B(k\tau) = \frac{6}{B_2^2 - B_1^2} \left[ \frac{\sin(B_1 k\tau)}{(B_1 k\tau)} - \frac{\sin(B_2 k\tau)}{(B_2 k\tau)} \right], \quad (16)$$

where  $0 < (B_1, B_2) < 1$  and we have normalized the function to behave as  $(k\tau)^2$  on small scales. Thus Eq. (13) and (16) represent the mode decompositions of a scaling isotropic and anisotropic stress perturbation which strictly obeys causal constraints for a lack of correlations above the horizon.

### III. IMPLICATIONS FOR THE CMB

#### A. Acoustic Sources and Signatures

Let us first review the formalism set up in [1] for calculating the acoustic oscillations in the CMB for a model with external gravitational sources. To avoid obscuring the main physical points, we have relegated the technical details to the Appendices A and B. The basic idea is that one solves the equations for the fluid and metric evolution under the influence of sources which are assumed to interact with the fluids only through gravity. For CMB studies, it is convenient to choose a Newtonian gauge condition to represent these effects, since the perturbations are more easily interpreted in this gauge than in the synchronous or comoving gauge. The Einstein equations tell us that the matter fields generate Newtonian metric perturbations: specifically the curvature  $\Phi$  and gravitational potential  $\Psi$ .

Under the methods of [1], the gravitational contributions of the photon-baryon fluid are separated from the other sources,  $\Phi = \Phi_{\gamma b} + \Phi_s$  and  $\Psi = \Psi_{\gamma b} + \Psi_s$ . The photon-baryon oscillator equation is then solved in the presence of  $\Phi_s$  and  $\Psi_s$ . If we assume that the source is composed of seeds, i.e. a component whose stress-energy tensor makes a small perturbation to the background, its contribution is [see Eqs. (A4) and (A11)]

$$\begin{aligned} (k^2 - 3K)\Phi_s &= 4\pi G a^2 (\rho_s + 3\frac{\dot{a}}{a} v_s / k), \\ k^2(\Psi_s + \Phi_s) &= -8\pi G a^2 \pi_s, \end{aligned} \quad (17)$$

where we have simply labeled the scalar terms of the stress-energy tensor of the seeds in the fluid convention without loss of generality<sup>1</sup> [see Eq. (A4)]. Thus since defect seeds merely represent a special case of an external source, they may easily be treated under this formalism.

---

<sup>1</sup>For reference, note that the relationship between [3,6] and our notation is  $\Theta_{00} = a^2 \rho_s$ ,  $\Theta_{ii} = 3a^2 p_s$ ,  $\Theta_S = -a^2 \pi_s$  and  $\Pi = -a^2 k v_s$ .

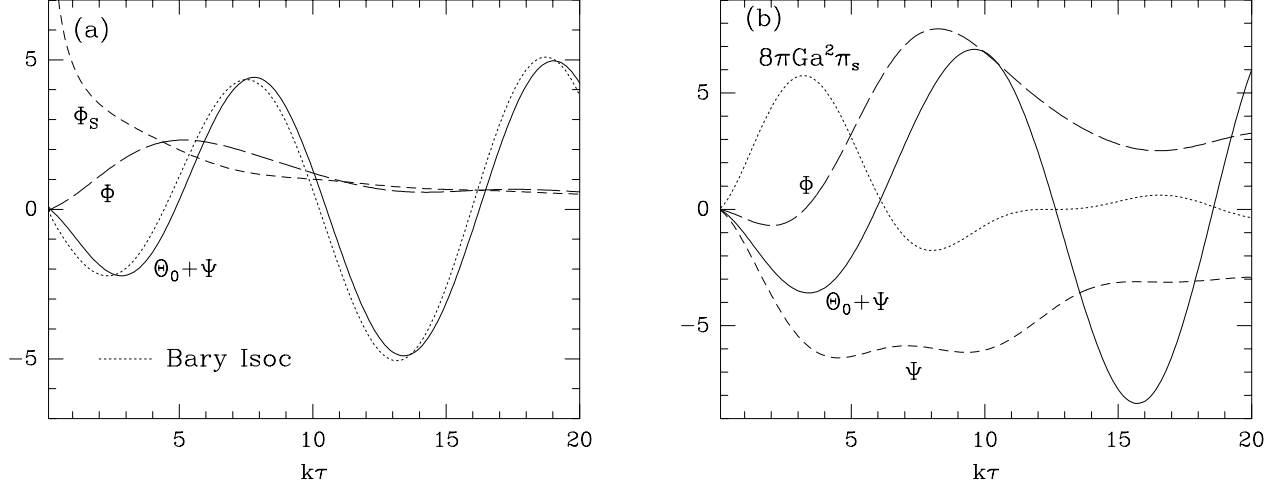


FIG. 1. (a) Pressure scaling source. The effective temperature  $\Theta_0 + \Psi$ , total curvature perturbation  $\Phi$ , and the contribution from the source  $\Phi_s$ , produced by  $p_s$  assuming Eq. (18) with  $A = 1$ . Notice that the temperature fluctuations are similar to the canonical prediction of a baryon-isocurvature model (dotted line), not inflation. (b) Anisotropic stress scaling source. Evolution under  $\pi_s$  assuming Eq. (19) with  $B_1 = 1$ ,  $B_2 = 0.5$ . Photon domination is assumed here and in Figs. 3 and 4.

To summarize the results of [1], it was established that isocurvature initial conditions, in the sense of §II B and Appendix B, robustly predict an anticorrelation between the source curvature and CMB temperature perturbations at horizon crossing during radiation domination. The underlying reason is obvious from the causal arguments of §II: changes in the source energy density must be compensated by an opposing change in the radiation density before bulk motion has had a chance to redistribute the matter. Since correlations and anticorrelations with the curvature represent compressions and rarefactions in potential wells respectively under normal conditions, the acoustic signature can distinguish between these cases (see §III D and Appendix C for exceptions). The specific signature is provided by the drag baryons induce on the photon-baryon fluid which enhances compressions over rarefactions. Thus the signature of an inflationary model is given by the ratio of the acoustic peak locations, which measures the phase of the acoustic oscillation, and an enhancement of the odd peak heights. It was found that though a distinctly different set of “sine” peak ratios was a common prediction of isocurvature models, details of the source evolution could be tuned to reproduce the inflationary case (see also [4]) so that the peak height test is also necessary. We now consider whether additional assumptions, such as scaling in a strictly causal stress model, can produce further robust distinctions.

### B. Scaling Ansatz for Pressure

Let us now specialize the analysis of [1] to the case where the source pressure fluctuations are from seeds that obey the scaling ansatz discussed in §II C. Specifically, let us break the pressure source into contributions that behave as

$$4\pi G a^2 p_s = \tau^{-1/2} f_A = \tau^{-1/2} \frac{\sin(Ak\tau)}{(Ak\tau)}, \quad (18)$$

with  $0 < A < 1$ . This choice is similar to and inspired by the ansatz of [6] but replaces the assumption for  $a^2(\rho_s + 3p_s)$  with the analogous one for  $a^2 p_s$  since stress fluctuations are the fundamental source of causally-seeded perturbations. This allows energy-momentum conservation to fix the form of density perturbations naturally from the stress fluctuations and permits a wider class of possible seed sources (see Appendix C). For simplicity, we here assume that the seed anisotropic stress  $\pi_s = 0$  and postpone discussion of its effect until the next section.

We show the evolution of the system under the source Eq. (18) in Fig. 1a. We have chosen  $A = 1$  since this is the most extreme of the causal modes in that it produces features in the source as soon as causally possible. The initial conditions require a vanishing comoving curvature  $\zeta = 0$  or equivalently vanishing stress-energy pseudo-tensor components  $\tau_{00} = 0 = \tau_{0i}$ . As long as the initial conditions are set early enough so that the pressure has not generated significant perturbations, this may be satisfied by setting the individual energy density and momentum

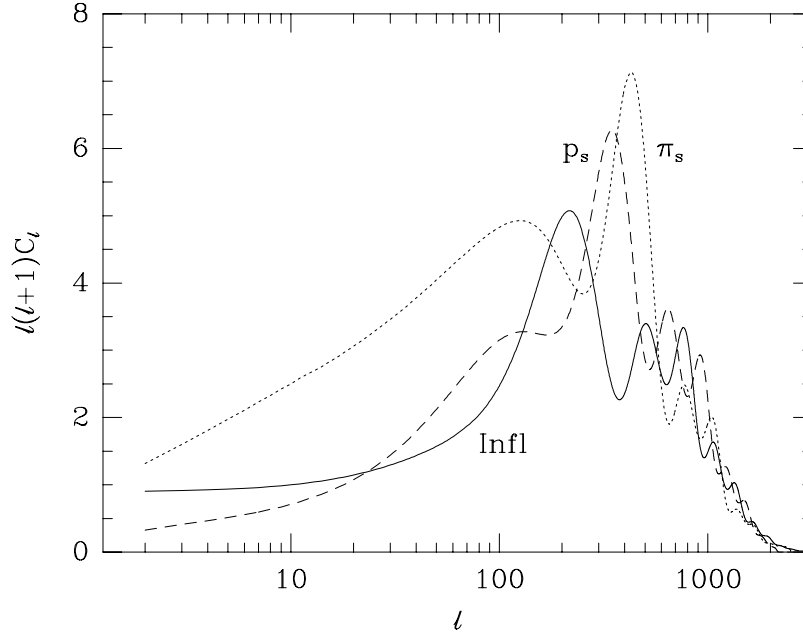


FIG. 2. The anisotropy power spectrum,  $\ell(\ell+1)C_\ell$ , vs multipole number  $\ell \sim \theta^{-1}$ . The solid line is the inflationary prediction. The dashed line assumes a pressure source with the form of Eq. (18) for  $A = 1$ . The dotted line assumes an anisotropic source with the form of Eq. (19) for  $B_1 = 1$  and  $B_2 = 0.5$ . All curves assume the same background cosmology  $\Omega_0 = 1$ ,  $h = 0.5$ ,  $\Omega_b h^2 = 0.0125$ . Notice that the predictions are out of phase and that even rather than odd peaks are prominent in the non-inflationary models.

density perturbations of the fluids and sources to zero. Note that in the more general context in which the source fluctuations are directly related to density fluctuations, one must be more careful in setting up consistent compensated initial conditions.

We make the important assumption here that the universe is radiation dominated as the fluctuation enters the horizon which we will discuss further below (see also [1]). Notice that this model follows the predictions of a canonical isocurvature model  $\Phi_s \propto (k\tau)^{-1}$  (e.g. a baryon or axion isocurvature model [1,10]), quite closely. Here the effective temperature perturbation  $\Theta_0 + \Psi$  is composed of the temperature fluctuation on Newtonian surfaces  $\Theta_0 = \delta_\gamma^N/4$  [see Eq. (A16)], and the Newtonian potential  $\Psi$  which accounts for the gravitational redshift or Sachs-Wolfe effect.

Note that the sign change in the pressure at  $k\tau = \pi$  has no direct relevance to the question of acoustic phase. The action of a source near or outside the horizon generically drives a sine mode acoustic wave due to feedback from the self-gravity of the photon-baryon fluid. The situation for which these arguments fail is if feedback is unimportant, i.e. if the universe is *fully* matter-dominated when the mode entered the horizon. These issues are treated in much greater detail in [1].

To demonstrate that this potential loophole is not a concern for reasonable cosmological parameters, we perform a full calculation of the  $A = 1$  model by solution of the complete Boltzmann equations (see e.g. [30]). Specifically, the model includes cold dark matter and three species of massless neutrinos with standard recombination and cosmological parameters of  $\Omega_0 = 1$ ,  $\Omega_0 h^2 = 0.25$ ,  $\Omega_b h^2 = 0.0125$ . Even if the matter-radiation density ratio at last scattering were as high as  $\rho_m/\rho_r \approx 16$ , as in this case, the acoustic signature remains distinctly isocurvature. In Fig. 2, we compare the power per log  $\ell \sim \theta^{-1}$  in anisotropies  $\ell(\ell+1)C_\ell$  for this model with the standard inflationary model for the same cosmological parameters. We have explicitly checked by the Boltzmann calculation that in a universe with the standard thermal history and reasonable matter content  $\Omega_0 h^2 \lesssim 1$ , the loophole provided by the absence of photon backreaction does not exist.

Note that the calculation of Fig. 2 also includes gravitational effects between last scattering and the present, i.e. the integrated Sachs-Wolfe (ISW) effect, in addition to the acoustic temperature fluctuation displayed in Fig. 1. It thus corresponds to the *physically observable* total anisotropy from the pressure fluctuations defined by the model. We comment on the importance of calculating the observable anisotropy in Appendix C.

It is interesting to consider the full range of  $0 < A < 1$  since the modes may be superimposed to produce a more



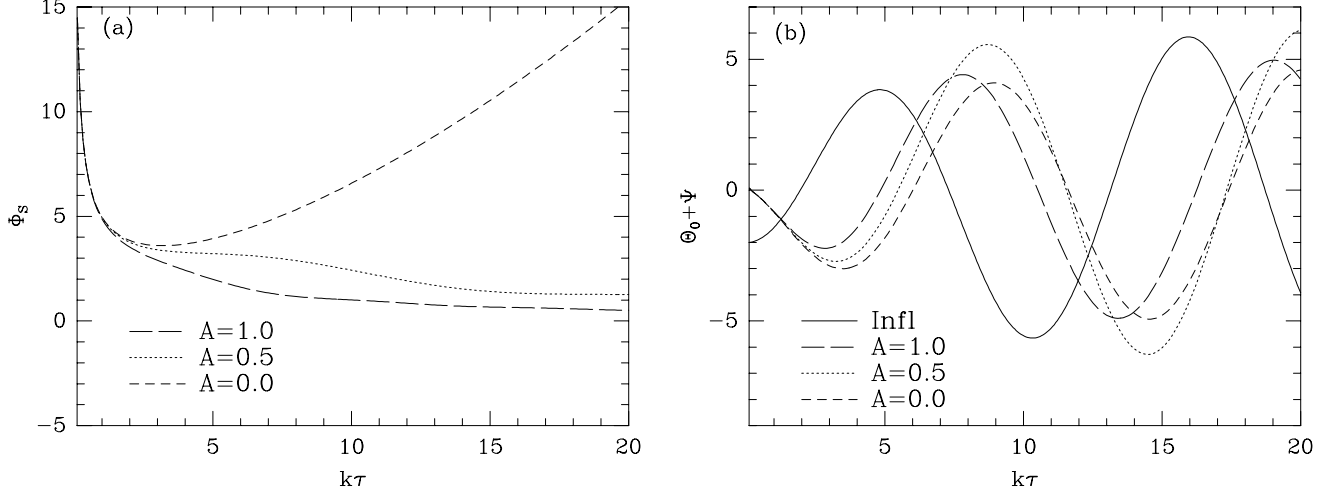


FIG. 3. We show (a) the source curvature  $\Phi_s$  and (b) the effective temperature  $\Theta_0 + \Psi$  for the family of pressure sources of Eq. (18). In all cases, the effective temperature approximately follows the canonical isocurvature evolution from Fig. 1, which is very different from the inflationary case (solid line in panel b).

general case. Fig. 3a shows that varying  $A$  dramatically changes the behavior of the curvature source inside the horizon ( $k\tau \geq 1$ ). The source falls rapidly, has a peak at  $k\tau_{\text{peak}} \propto A^{-1}$ , then falls again. On the other hand, when one examines its effect on the photon-baryon fluid in Fig. 3b, the change with  $A$  is much less dramatic. In fact for all  $0 < A < 1$ , the acoustic oscillations follow the isocurvature pattern of a near sine mode with even compressional (positive) peaks. This result is also easy to understand from [1]. It is far easier to stimulate an acoustic mode as the fluctuation crosses the Jeans scale (i.e. the sound horizon) than after it. Even the dramatic changes in the curvature inside the horizon shown in Fig. 3 are not sufficient to overwhelm the signal created at crossing. These arguments apply to any slowly-varying source of metric fluctuations inside the horizon. It is possible to obtain somewhat more rapidly-varying features by interfering different  $A$  modes. This may occur if additional symmetries in the source eliminate the white noise pressure contributions (see Appendix B 2) and produces effects similar to anisotropic stress sources considered in the next section [cf. Eqs. (13) and (16)]. One should also be careful in that although this acoustic signature is robust for individual  $A$  modes, it may be difficult to observe in the low  $A \lesssim 0.3$  case. Since after last scattering potential fluctuations eventually decay, additional contributions from the ISW effect can mask this signal. They do not however possess oscillatory features and hence cannot be employed to mimic the inflationary spectrum.

Thus we come to the conclusion that this whole class of pressure scaling models produces an acoustic signature that bears the canonical isocurvature stamp: a sine mode oscillation with a rarefaction-compression-rarefaction pattern that leads to even peak enhancement from the baryons. Both properties are sufficiently distinctive so as not to be confused with inflation. This makes the task of distinguishing them simpler than in the general case [1] and renders them testable by the current generation of CMB experiments.

### C. Scaling Ansatz for Anisotropic Stress

Now let us consider the effect of anisotropic stress sources that obey the scaling ansatz. These sources are represented by the basis of Eq. (16),

$$4\pi G a^2 \pi_s = \tau^{-1/2} f_B = \tau^{-1/2} \frac{6}{B_2^2 - B_1^2} \left[ \frac{\sin(B_1 k\tau)}{(B_1 k\tau)} - \frac{\sin(B_2 k\tau)}{(B_2 k\tau)} \right]. \quad (19)$$

Anisotropic stress affects the CMB in two ways. It contributes directly to the gravitational potential  $\Psi$  through Eq. (14) and hence the Sachs-Wolfe effect. It also acts as a force in the momentum conservation equation [e.g. Eq. (1)] that moves matter around. Thus it generates true density and curvature fluctuations inside the horizon in the same way as the pressure perturbations.

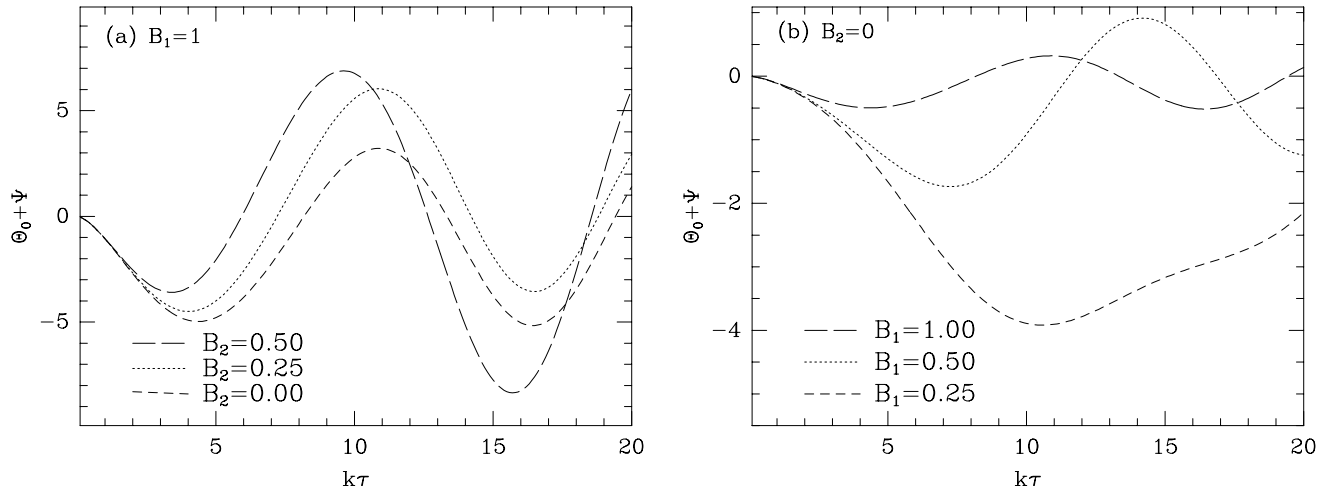


FIG. 4. Anisotropic stress scaling source time evolution (a)  $B_2$  controls the decline of  $\pi_s$  from its maximum and has little effect on the acoustic features. (b)  $B_1$  controls the location of the main peak in  $\pi_s$  and hence the location of the main acoustic feature.

The form of Eq. (19) implies that it is a source of white noise fluctuations in  $\Psi$  above the horizon. Due to the  $(k\tau)^2$  factor, we expect that the formation of acoustic oscillations by anisotropic stresses is delayed compared with formation by pressure fluctuations. This shifts the acoustic features toward smaller scales and further away from the predictions of inflation. On the other hand, their relatively late formation implies that the feedback mechanism from the compensating energy density of the photons at Jeans length crossing is less important leading to a wider range of possible effects in the CMB anisotropy spectrum.

Let us consider a few specific examples. In Fig. 1b, we show the time evolution of fluctuations in the photon-dominated era from an anisotropic stress of the form in Eq. (19) with  $B_1 = 1$  and  $B_2 = 0.5$ . As the anisotropic stress source turns on at  $k\tau \sim B_1^{-1}$ , it acts as a direct source of potential fluctuations  $\Psi$ . It then begins to move matter around. This produces significant density and accompanying curvature perturbations which thereafter dominate the structure of the gravitational potentials, i.e.  $\Psi \sim -\Phi$ . The result is an effective temperature  $\Theta_0 + \Psi$  that first follows  $\Psi$  into a rarefaction stage. The fluid then turns around to fall into the growing potential wells of the source. Thus the qualitative effect of anisotropic stress on the CMB is the same as isotropic stress: the feature at Jeans crossing corresponds to a rarefaction in the effective temperature and is suppressed in comparison to the main compressional feature due to infall into the potential well of the source. This expectation is borne out by the full Boltzmann calculation in Fig. 2. Because the dynamical effects of anisotropic stress are highly suppressed outside the horizon, the main features of the peaks are shifted toward smaller scales than for the pressure model.

Now let us consider how these results change with the form of the anisotropic stress source. The parameters  $B_1$  and  $B_2$  that define the anisotropic stress  $\pi_s$  in Eq. (19) control the maximum of  $\pi_s$  and the rapidity of its subsequent decline respectively. Here we have assumed that  $B_1 > B_2$ . In Fig. 4, we show how the time evolution of the effective temperature varies with  $B_1$  and  $B_2$ . Notice that altering the rapidity of the fall off through  $B_2$  has little effect on the acoustic structure whereas decreasing  $B_1$  shifts the main features toward later times and hence smaller scales. Thus the anisotropic stress models which have features closest to those of inflation set  $B_1 = 1$ .

Thus, we can conclude that anisotropic stress fluctuations tend to shift the main features toward smaller scales. Like the result for pressure fluctuations, this implies that any feature that is near the first peak in an inflationary model must be sub-dominant, leading to a low-high-low prediction for the heights of the features (see Fig. 2). As such, these models are easily distinguished from inflation.

#### D. Underlying Assumptions

Since the effects of causal pressure and anisotropic stress fluctuations are both individually distinguishable from those of inflation, one expects that the combination of the two would result in a spectrum equally distinguishable

unless there is interference between the modes. To better quantify our intuition and identify possible loopholes, it is instructive to recall the physical basis for the differences in the CMB spectra.

The crucial distinction between all of these isocurvature models and the inflation is the behavior of the fluctuations during horizon crossing. In an isocurvature model, any source density fluctuations at this epoch must be compensated to keep the total density fluctuation small. If the photons take part in this compensation, as they must if they are the dominant dynamical component at the epoch of horizon crossing, this implies an anticorrelation between the source and photon density fluctuations. Inflationary models generate adiabatic fluctuations so that the density fluctuations of all the species are correlated at horizon crossing. This leads to observable consequences with the *additional* assumption that overdense regions of the source represent gravitational potential wells. The Compton drag of the baryons on the photons attempts to compress the photon-baryon fluid in the potential well. In inflationary models, the photons are already overdense inside the well such that this effect enhances the first peak and subsequently all odd (compressional) peaks. In isocurvature models, the opposite occurs leading to a reduction of the first (rarefaction) peak and an enhancement of the second and all even peaks.

There are two basic assumptions to this chain of reasoning. The first is that the photons must play a role in the causal compensation. It is possible to construct a model in which the universe is fully matter dominated at horizon crossing for all observable peaks where this assumption is invalid [1]. However, we have shown in §III B that this does not occur in a model with the standard thermal history and reasonable cosmological parameters. The second assumption is that overdense regions of the source, here taken to mean all contributions external to the photon-baryon system, represent potential wells. This is generally a reasonable assumption even in the isocurvature case since the ability of the photon-density perturbation to counteract the source is diminished as the fluctuation passes the Jeans length. Thus source overdensities represent total overdensities. The Poisson equation implies that overdensities represent positive curvature fluctuations and hence potential wells *if* the anisotropic stress is negligible in comparison to the density fluctuation [see Eq. (14)].

The latter assumption opens up the possibility that anisotropic stress provides a loophole to these arguments. More specifically, if  $\pi_s > -\rho_s/2$ , then *underdense* regions of the source represent potential wells and the above expectation for the relative heights of the peaks is inverted. However, this does not occur if we just simply take a model with large anisotropic stress  $\pi_s$  (see §III C). The reason is that a large anisotropic stress moves matter around to create a correspondingly large density perturbation. The energy-momentum conservation laws for a seed source [from Eq. (A11) for wavelengths well below the background curvature scale]

$$\begin{aligned}\dot{\rho}_s + 3\frac{\dot{a}}{a}(\rho_s + p_s) &= -kv_s, \\ \dot{v}_s + 4\frac{\dot{a}}{a}v_s &= kp_s - \frac{2}{3}k\pi_s,\end{aligned}\tag{20}$$

imply that for  $k\tau \gg 1$ ,  $\pi_s$  is typically a strong source of density fluctuations.

Can we ever construct a model in which  $\pi_s \gtrsim -\rho_s/2$ ? An exception to the above arguments occurs if  $p_s = 2\pi_s/3$ . The stresses are then so balanced as to maintain a large anisotropic stress without generating a correspondingly large density perturbation (see discussion of Fig. 1). It is *not* sufficient to have merely  $\pi_s = \mathcal{O}(p_s)$  to achieve this balance.

For this one exceptional case, it is possible here to have gravitational potentials generated by anisotropic stress instead of density perturbations. If such a model additionally has the peaks in the inflationary positions *and* yields approximately constant gravitational potential perturbations, it is possible to evade the arguments of Hu & White [1]. Even though the individual effects of pressure and anisotropic stress fluctuations lead to predictions in accord with the canonical isocurvature model, the two may cancel in this way to evade such expectations. Following Turok [9], we explicitly construct such an example in Appendix C. Such models rely on a special relation between the pressure, anisotropic stress and density fluctuations and are thus unstable to perturbations in the equation of state [see discussion surrounding Eq. (C7)].

In summary, the two assumptions underlying the case for the distinguishability of inflation from isocurvature models from the acoustic signature are that the photons are dynamically significant at Jeans crossing and that potential wells represent overdense regions in space. These criteria are satisfied by a wide range of models including all those currently under consideration involving defects which have observable acoustic signatures.

## IV. DISCUSSION

All of the causal models for the formation of large scale structure currently being considered can be divided into two classes: (a) inflationary models, which have curvature fluctuations on superhorizon scales and (b) scaling

seeded-models, such as strings and textures. In the latter case, there are no initial curvature fluctuations and stress fluctuations only generate them through the causal redistribution of matter under energy-momentum conservation [7,8].

We have presented a thorough discussion of this process that can be used to study the general properties of any model that proposes a causal mechanism for large scale structure formation without postulating an inflationary epoch. We apply these techniques to study a representative class of scaling models inspired by Turok [6]. For models dominated by white noise isotropic stress fluctuations, the acoustic signature in the CMB angular power spectrum follows the canonical signature of a baryon-isocurvature model. Physically, this robust signature arises from the ability of photon-backreaction to drive the acoustic oscillation [1], a feature that must be included in a self-consistent calculation. Models dominated by anisotropic stress fluctuations tend to be even more extreme, with main features pushed toward smaller scales. Hence both classes are easily distinguished from inflation by experiments currently underway (see Fig. 3).

A realistic model, such as strings or textures, may contain additional complications beyond the simple toy-models explored in this paper, such as tensor and vector contributions as well as reionization. It can also require non-linear evolution of the sources that couple the normal modes discussed here and leave non-gaussian signatures in the CMB and/or cause decoherence in the oscillation [4]. However, such complications are likely to make alternate models less, rather than more, like inflation.

The analysis in this paper also reinforces the conclusions of [1]: in an inflationary model, even peaks are produced by rarefaction waves and odd peaks are produced by compression waves. On the other hand in isocurvature models, even peaks are produced by compression waves and odd peaks are produced by rarefaction waves. As long as the energy density in radiation at decoupling is significant and gravitational potential wells represent overdense regions, such a model cannot reproduce the inflationary CMB signature without the equivalent of putting in the features by hand.

*Acknowledgements:* We thank J.N. Bahcall, P.G. Ferreira and A. Stebbins for useful discussions, as well as D. Scott, N.G. Turok, and J. Magueijo for comments on a draft of this work. W.H. was supported by the NSF and WM Keck Foundation.

## APPENDIX A: RELATIVISTIC PERTURBATION THEORY WITH SEEDS

We review the formalism of relativistic perturbation theory in this appendix and derive the results used in the main text. We start with a discussion of gauge transformations in general relativistic perturbation theory and then derive the metric evolution and fluid equations in three commonly employed gauges (see also [16,32]). Each of these gauges has advantages for particular problems we consider in the text, and we present all of the details necessary to transform from one to the other.

### 1. Gauge Transformations

The most general form of a metric perturbed by scalar fluctuations is [7,8]

$$\begin{aligned} g_{00} &= -a^2[1 + 2A^G Q], \\ g_{0j} &= -a^2 B^G Q_j, \\ g_{ij} &= a^2[\gamma_{ij} + 2H_L^G Q \gamma_{ij} + 2H_T^G Q_{ij}], \end{aligned} \tag{A1}$$

where  $Q$  is the  $k$ th eigenfunction of the Laplacian, *i.e.*  $\exp(i\mathbf{k} \cdot \mathbf{x})$  in a flat space,  $Q_i \equiv -k^{-1}Q_{|i}$  and  $Q_{ij} = k^{-2}Q_{|ij} + \gamma_{ij}Q/3$  where  $|$  denotes a covariant derivative with respect to the background 3-metric  $\gamma_{ij}$  of constant curvature  $K = -H_0^2(1 - \Omega_0 - \Omega_\Lambda)$ . The superscript  $G$  is employed to remind the reader that the actual values vary from gauge to gauge.

A gauge transformation is a change in the correspondence between the perturbation and the background represented by the coordinate shifts

$$\begin{aligned} \tilde{\tau} &= \tau + TQ, \\ \tilde{x}^i &= x^i + LQ^i, \end{aligned} \tag{A2}$$

where the conformal time  $\tau$  is defined through  $d\tau = dt/a(t)$  with  $a$  as the scale factor.  $T$  corresponds to a choice in time slicing and  $L$  a choice of spatial coordinates. Under the condition that metric distances be invariant, they transform the metric as [8]

$$\begin{aligned} A^{\tilde{G}} &= A^G - \dot{T} - \frac{\dot{a}}{a}T, \\ B^{\tilde{G}} &= B^G + \dot{L} + kT, \\ H_L^{\tilde{G}} &= H_L^G - \frac{k}{3}L - \frac{\dot{a}}{a}T, \\ H_T^{\tilde{G}} &= H_T^G + kL. \end{aligned} \tag{A3}$$

The normal mode decomposition of the scalar part of the stress-energy tensor for a fluid ( $f$ ) plus seed source ( $s$ ) yields

$$\begin{aligned} T_0^0 &= -\rho_f - (\rho_f \delta_f^G + \rho_s)Q, \\ T_i^0 &= [(\rho_f + p_f)(v_f^G - B^G) + v_s]Q_i, \\ T_0^i &= -[(\rho_f + p_f)v_f^G + v_s]Q_i, \\ T_j^i &= [p_f + (\delta p_f^G + p_s)Q]\delta_j^i + (p_f \pi_f^G + p_s)Q_j^i. \end{aligned} \tag{A4}$$

It is occasionally convenient to break the fluid up into its various particle components, *e.g.*  $\rho_f \delta_f \rightarrow \sum_f \rho_f \delta_f = \rho_T \delta_T$ , and we shall preserve generality by writing equations applicable to either the single- or multi-fluid case. The gauge transformations act on the fluid quantities as [8]

$$\begin{aligned} v_f^{\tilde{G}} &= v_f^G + \dot{L}, \\ \delta_f^{\tilde{G}} &= \delta_f^G + 3(1 + w_f)\frac{\dot{a}}{a}T, \\ \delta p_f^{\tilde{G}} &= \delta p_f^G + 3c_f^2 \rho_f (1 + w_f)\frac{\dot{a}}{a}T, \\ \pi_f^{\tilde{G}} &= \pi_f^G, \end{aligned} \tag{A5}$$

whereas for the seed source they only generate second order corrections. Here  $w_f = p_f/\rho_f$  defines the equation of state,  $c_f^2 = \dot{p}_f/\dot{\rho}_f$  is the sound speed in the fluid, and we have used  $\dot{\rho}_f/\rho_f = -3(1+w_f)(\dot{a}/a)$ . Notice that the anisotropic stress  $\pi_f$  has a truly gauge invariant meaning, and we shall hereafter drop the superscript  $G$  from it.

## 2. Synchronous Gauge

Let us derive the energy-momentum conservation and Einstein-Poisson equations in the familiar synchronous gauge and use the gauge transformation above to relate them to alternate representations. The synchronous gauge is defined by  $A^S = B^S = 0$  implying that proper time corresponds with coordinate time and that constant spatial coordinates are orthogonal to constant time hypersurfaces, a natural coordinate system for freely-falling observers. From any other coordinate system, it is reached by the transformation

$$\begin{aligned} T &= a^{-1} \int d\tau a A^G + c_1 a^{-1}, \\ L &= - \int d\tau (B^G + k T^G) + c_2, \end{aligned} \quad (\text{A6})$$

where the presence of the integration constants  $c_1$  and  $c_2$  reflects the fact that the synchronous condition does not uniquely fix the coordinates. In the past, this fact has lead to much confusion since coordinate ambiguity in  $T$  appears as a fictitious gauge mode in the density evolution. It is conventional to define

$$\begin{aligned} h &= 6H_L^S, \\ \eta &= -H_L^S - \frac{1}{3}H_T^S, \end{aligned} \quad (\text{A7})$$

as the fundamental metric variables. Covariant conservation of the stress-energy contributions of the fluid yields the continuity equation for the background  $\dot{\rho}_f = -3(\rho_f + p_f)(\dot{a}/a)$  and for the perturbations

$$\frac{d}{d\tau} \left( \frac{\delta_f^S}{1+w_f} \right) = -(k v_f^S + \dot{h}/2) - 3 \frac{\dot{a}}{a} \frac{w_f}{1+w_f} \Gamma_f, \quad (\text{A8})$$

as well as the Euler equation

$$\dot{v}_f^S + \frac{\dot{a}}{a} (1 - 3c_f^2) v_f^S = \frac{c_f^2}{1+w_f} k \delta_f^S + \frac{w_f}{1+w_f} k \Gamma_f - \frac{2}{3} \frac{w_f}{1+w_f} (1 - 3K/k^2) k \pi_f. \quad (\text{A9})$$

Here, the non-adiabatic pressure perturbation or “entropy” fluctuation is defined as

$$p_f \Gamma_f = \delta p_f^G - c_f^2 \delta \rho_f^G, \quad (\text{A10})$$

and is manifestly gauge invariant [Eq. (A5)]. Likewise, conservation of the seed source gives the equations

$$\begin{aligned} \dot{\rho}_s + 3 \frac{\dot{a}}{a} (\rho_s + p_s) &= -k v_s, \\ \dot{v}_s + 4 \frac{\dot{a}}{a} v_s &= k p_s - \frac{2}{3} k (1 - 3K/k^2) \pi_s, \end{aligned} \quad (\text{A11})$$

which are also manifestly gauge invariant.

In this gauge, the Einstein equations are straightforward to derive. The evolution of the scale factor is determined by

$$\left( \frac{\dot{a}}{a} \right)^2 + K = \frac{8\pi G}{3} a^2 \rho_T, \quad (\text{A12})$$

and the metric perturbations are given in terms of the matter sources as<sup>2</sup>

---

<sup>2</sup>In [33] there is a typographical error in Eq. (A16) and the first of Eq. (A45). These equations are missing a minus sign. No results are changed.

$$\begin{aligned}
(k^2 - 3K)\eta - \frac{\dot{a}}{a} \frac{\dot{h}}{2} &= -4\pi G a^2 [\delta_T^S \rho_T + \rho_s], \\
k\dot{\eta} - \frac{K}{2k}(\dot{h} + 6\dot{\eta}) &= 4\pi G a^2 [(\rho_T + p_T)v_T^S + v_s], \\
\ddot{h} + \frac{\dot{a}}{a} \dot{h} &= -8\pi G a^2 [\delta_T^S \rho_T + 3\delta p_T^S + \rho_s + 3p_s], \\
\ddot{h} + 6\ddot{\eta} + 2\frac{\dot{a}}{a}(\dot{h} + 6\dot{\eta}) - 2k^2\eta &= -16\pi G a^2 [p_T \pi_T + \pi_s].
\end{aligned} \tag{A13}$$

Notice that the third equation implies that  $h$ , unlike  $\eta$ , is dependent only on  $\rho + 3p$ .

### 3. Newtonian Gauge

The Newtonian gauge is defined by the sheer free condition  $B^N = H_T^N = 0$ , and it is conventional to call the remaining metric variables the Newtonian potential  $\Psi \equiv A^N$  and curvature fluctuation  $\Phi \equiv H_L^N$ . From an arbitrary gauge, it is reached by the transformation

$$\begin{aligned}
T &= -B^G/k + \dot{H}_T^G/k^2 \quad [= -\frac{1}{2}(\dot{h} + 6\dot{\eta})/k^2], \\
L &= -H_T^G/k \quad [= \frac{1}{2}(h + 6\eta)/k],
\end{aligned} \tag{A14}$$

where we have also specialized it to synchronous gauge in the square brackets. Thus the Newtonian metric perturbations can be written in terms of their synchronous counterparts as

$$\begin{aligned}
\Psi &= \frac{1}{2}[\ddot{h} + 6\ddot{\eta} + \frac{\dot{a}}{a}(\dot{h} + 6\dot{\eta})]/k^2, \\
\Phi &= -\eta + \frac{1}{2}\frac{\dot{a}}{a}(\dot{h} + 6\dot{\eta})/k^2,
\end{aligned} \tag{A15}$$

and likewise for the fluid variables

$$\begin{aligned}
\delta_f^N &= \delta_f^S - \frac{3}{2}(1 + w_f)\frac{\dot{a}}{a}(\dot{h} + 6\dot{\eta})/k^2, \\
\delta p_f^N &= \delta p_f^S - \frac{3}{2}c_f^2 \rho_f (1 + w_f)\frac{\dot{a}}{a}(\dot{h} + 6\dot{\eta})/k^2, \\
v_f^N &= v_f^S + \frac{1}{2}(\dot{h} + 6\dot{\eta})/k.
\end{aligned} \tag{A16}$$

It is a straightforward exercise in algebra to transform the synchronous gauge equations. The conservation equations become

$$\begin{aligned}
\frac{d}{d\tau} \left( \frac{\delta_f^N}{1 + w_f} \right) &= -(k v_f^N + 3\dot{\Phi}) - 3\frac{\dot{a}}{a} \frac{w_f}{1 + w_f} \Gamma_f, \\
\dot{v}_f^N + \frac{\dot{a}}{a}(1 - 3c_f^2)v_f^N &= \frac{c_f^2}{1 + w_f} k \delta_f + \frac{w_f}{1 + w_f} k \Gamma_f - \frac{2}{3} \frac{w_f}{1 + w_f} (1 - 3K/k^2) k \pi_f + k \Psi,
\end{aligned} \tag{A17}$$

and Einstein-Poisson equations become,

$$\begin{aligned}
(k^2 - 3K)\Phi &= 4\pi G a^2 \left\{ \rho_T \delta_T^N + \rho_s + 3\frac{\dot{a}}{a}[(\rho_T + p_T)v_T^N + v_s]/k \right\}, \\
k^2(\Psi + \Phi) &= -8\pi G a^2 (p_T \pi_T + \pi_s).
\end{aligned} \tag{A18}$$

It is also useful to note that the gauge transformation properties imply that from an arbitrary gauge, the Newtonian potential can be constructed as

$$(k^2 - 3K)\Phi = 4\pi G a^2 \left( \delta_T^G \rho_T + 3\frac{\dot{a}}{a}[(\rho_T + p_T)(v_T^G - B^G) + v_s]/k \right), \tag{A19}$$

which is commonly called the gauge-invariant Poisson equation.

#### 4. Comoving Gauge

The comoving gauge (superscript  $T$ ) is defined by the vanishing of the energy density flux  $T^0_i = 0$  and the auxiliary condition  $H_T^T = 0$ . It is also sometimes called the velocity-orthogonal isotropic gauge, the total-matter gauge and the rest frame gauge. For convenience, we denote  $\xi \equiv A^T$  and  $\zeta \equiv H_L^T$ . From an arbitrary gauge, it is reached by

$$\begin{aligned} T &= [v_T^G + v_s/(\rho_T + p_T) - B^G]/k & [= \{v_T^S + v_s/(\rho_T + p_T)\}/k], \\ L &= -H_T^G/k & [= \frac{1}{2}(h + 6\eta)/k], \end{aligned} \quad (\text{A20})$$

where we have again also specialized to synchronous gauge and used the notation  $(\rho_T + p_T)v_T = \sum_f(\rho_f + p_f)v_f$  to preserve generality in the multifluid case. The gauge transformations imply that

$$\begin{aligned} \zeta &= \Phi - \frac{\dot{a}}{a}[v_T^N + v_s/(\rho_T + p_T)]/k \\ &= -\eta - \frac{\dot{a}}{a}[v_T^S + v_s/(\rho_T + p_T)]/k, \end{aligned} \quad (\text{A21})$$

and the comoving density is defined as

$$\delta_f^T = \delta_f^S + 3(1 + w_f)\frac{\dot{a}}{a}[v_T^S + v_s/(\rho_T + p_T)]/k. \quad (\text{A22})$$

Note that the rhs is the same if we employ the Newtonian gauge density and velocity perturbation. Since the velocity is the same as in the Newtonian gauge  $v_f^T = v_f^N$ , we obtain for the conservation equations

$$\begin{aligned} \frac{d}{d\tau} \left( \frac{\delta_f^T}{1 + w_f} \right) &= -(kv_f^T + 3\dot{\zeta}) - 3\frac{\dot{a}}{a}\frac{w_f}{1 + w_f}\Gamma_f, \\ v_f^T + \frac{\dot{a}}{a}(1 - 3c_f^2)v_f^T &= \frac{c_f^2}{1 + w_f}k\delta_f^T - 3\frac{\dot{a}}{a}c_T^2[v_T^T + v_s/(\rho_T + p_T)] \\ &\quad + \frac{w_f}{1 + w_f}k\Gamma_f - \frac{2}{3}\frac{w_f}{1 + w_f}(1 - 3K/k^2)k\pi_f \\ &\quad - \frac{k}{k^2 - 3K}4\pi Ga^2(\rho_T\delta_T^T + \rho_s) - 8\pi Ga^2(p_T\pi_T + \pi_s)/k. \end{aligned} \quad (\text{A23})$$

The evolution of the metric perturbations can be obtained from the relations (A13) and (A9) for the synchronous Poisson and Euler equations

$$\begin{aligned} \xi &= -S/(\rho_T + p_T), \\ \dot{\zeta} &= \frac{\dot{a}}{a}\xi - K[v_T^T + v_s^T/(\rho_T + p_T)]/k, \end{aligned} \quad (\text{A24})$$

where the fundamental source to metric fluctuations is given by the stress perturbations

$$\begin{aligned} S &= c_T^2\rho_T\delta_T^T + p_T\Gamma_T + p_s - \frac{2}{3}(1 - 3K/k^2)(p_T\pi_T + \pi_s) \\ &= \delta p_T^T + p_s - \frac{2}{3}(1 - 3K/k^2)(p_T\pi_T + \pi_s). \end{aligned} \quad (\text{A25})$$

The fact that stress perturbations act as the direct source of comoving curvature is important for the causal arguments we make in §II.

#### APPENDIX B: CAUSAL CONSTRAINTS

Once the stress fluctuations are known, the causal evolution of matter and metric fluctuations is determined by energy momentum conservation and the Einstein-Poisson equations respectively. Thus to impose causality on a model, one must merely ensure that the initial conditions are causal and enforce causal stress perturbation behavior. In this appendix, we shall consider these two issues in detail.



## 1. Initial Conditions

If the initial conditions could be set up when the metric of the universe was precisely Friedman-Robertson-Walker, they are trivial: zero perturbations in all quantities initially, independent of complications such as gauge. Realistically however, we can only start the calculation some finite time afterwards when stress fluctuations and consequently some metric, energy density and momentum density fluctuations have already formed. As is evident from Appendix A, covariant energy-momentum conservation, and hence the causal constraint on these quantities, takes on different forms in different gauges. It is useful to pick a representation that corresponds to our naive intuition for causal evolution discussed in §II: that these three quantities should be negligibly small near the initial epoch well outside the horizon (see also Appendix of [1]).

We can summarize this intuition as follows: pressure gradients can cause a change in the momentum density of the matter and hence a bulk velocity of order  $(k\tau)\delta p/(p + \rho)$ . The divergence of the bulk velocity then kinematically forms a density perturbation of order  $(k\tau)^2\delta p/(p + \rho)$  corresponding to a curvature fluctuation of order  $\delta p/(p + \rho)$  from the Poisson equation. The fact that this process requires the movement of matter sets the causal constraint that the energy density fluctuation, momentum density and curvature fluctuation all must vanish initially. However, this intuition only holds if metric terms in the energy-momentum conservation equations leave the basic form of the conservation equations unaltered.

The comoving gauge provides the desired representation. If we assume that the wavelength of the fluctuation is much less than the curvature scale of the background, as we shall throughout this section, Eq. (A24) implies that the curvature perturbation  $\zeta$  in this gauge only changes under the influence of stress sources, exactly as we would naively expect. In the absence of stress sources  $\dot{\zeta} = 0$  and the continuity equation of Eq. (A23) reduces to an ordinary conservation law for number density fluctuations in a fluid:  $(\delta n_f^T/n_f) \propto \delta_f^T/(1 + w_f)$  and  $d(\delta n_f^T/n_f)/d\tau = -kv_f^T$ . Furthermore in this gauge we can rewrite Eq. (A23) purely in terms of the stresses [using Eq. (A24)], making manifest the intuition developed earlier regarding stresses as the generators of velocities and thus density perturbations. The continuity equation for the combined fluid and source components becomes

$$\frac{d}{d\tau} \left( \frac{\delta_T^T \rho_T + \rho_s}{\rho_T + p_T} \right) = -k[v_T^T + v_s/(\rho_T + p_T)] + 3\frac{\dot{a}}{a}F, \quad (\text{B1})$$

where

$$(\rho_T + p_T)F = c_T^2[\delta_T^T \rho_T + \rho_s] - \frac{2}{3}(p_T\pi_T + \pi_s). \quad (\text{B2})$$

Note that the adiabatic pressure term  $\propto c_T^2$  is proportional to the density perturbations and is thus initially ineffective. Furthermore, anisotropic terms are generically suppressed by  $k^2$  compared with pressure terms outside the horizon. Thus Eq. (B1) implies that energy density perturbations in this gauge are built up initially by energy density flows. Combined with the stress sources from the Euler equation, this implies that  $\delta_T^T \rho_T + \rho_s$  will build a tail that scales as  $(k\tau)^2(\delta p_T^T + p_s)$  for  $k\tau \ll 1$  as expected. Thus our intuition as to the nature of the causal constraint can be carried directly over to the comoving gauge, unlike the synchronous and Newtonian gauges where the total density fluctuation is not suppressed by  $(k\tau)^2$  with respect to the pressure fluctuation outside the horizon.

In comoving gauge, the causal constraint is imposed by assuming that the curvature  $\zeta = 0$  initially. The above arguments also show that setting the comoving total density to zero initially is essentially equivalent though slightly more restrictive as we shall show below. For calculational purposes, it is convenient to represent this constraint in other gauges. Recall that the  $\zeta$  curvature is constructed from synchronous gauge perturbations as

$$k\zeta = -k\eta - \frac{\dot{a}}{a}[v_T^S + v_s/(\rho_T + p_T)], \quad (\text{B3})$$

where as stated above we ignore factors of  $K/k^2$  throughout this section. To shed more light on this condition, it is useful to recall how energy flux generates metric perturbations in this gauge [see Eq. (A13)],

$$k\dot{\eta} = 4\pi G a^2[(\rho_T + p_T)v_T^S + v_s]. \quad (\text{B4})$$

Notice if we make the assignment

$$\begin{aligned} \tau_{00} &\equiv -(k^2\eta/4\pi G)Q = [\delta_T^S a^2 \rho_T + a^2 \rho_s - \frac{1}{8\pi G} \frac{\dot{a}}{a} \dot{\eta}]Q, \\ \tau_{0i} &\equiv a^2[(\rho_T + p_T)v_T^S + v_s](i\hat{k}_i)Q, \end{aligned} \quad (\text{B5})$$

Eq. (B4) takes on the form of a conservation equation

$$\dot{\tau}_{00} = \partial^i \tau_{0i}. \quad (\text{B6})$$

In the literature, this quantity is called the stress-energy pseudo-tensor [16] and is ordinarily rather than covariantly conserved. It is easy to see from Eq. (B3) that the vanishing of the  $\zeta$  curvature initially is equivalent to the statement that  $\tau_{00} = 0$  and  $\tau_{0i} = 0$ , i.e. that the pseudo-energy perturbation and the pseudo-momentum-density vanish initially as one would expect for conserved quantities. Thus the two sets of initial conditions are entirely equivalent.

Finally, let us consider the initial conditions for the Newtonian gauge. From Eq. (A19), the Newtonian curvature  $\Phi$  is algebraically related to the comoving gauge densities as

$$(k^2 - 3K)\Phi = 4\pi G a^2 (\rho_T \delta_T^T + \rho_s). \quad (\text{B7})$$

This implies that the isocurvature condition in the comoving gauge  $\zeta = 0$  should be directly related to the isocurvature condition in Newtonian gauge (see also discussion in [1]). Let us rewrite Eq. (A21) using the Newtonian continuity equation (A17) and the derivative of the Poisson equation (A18) as [22]

$$\zeta = \Phi + \frac{2}{3} \frac{1}{1 + w_T} \left( \frac{a}{\dot{a}} \dot{\Phi} - \Psi \right). \quad (\text{B8})$$

If anisotropic stress vanishes initially, the equation of state of the background is constant and  $\Phi$  evolves as a power law then  $\zeta \propto \Phi$ . The two curvature fluctuations are comparable except in the degenerate case where  $\zeta = 0$  and

$$\frac{\dot{\Phi}}{\Phi} = -\frac{\dot{a}}{a} \left[ \frac{3}{2} (1 + w_T) + 1 \right]. \quad (\text{B9})$$

In the radiation dominated era,  $w_T = 1/3$  and this represents a mode that decays as  $\Phi \propto \tau^{-3}$ . Thus the condition  $\zeta = 0$  is equivalent to  $\Phi = 0$  except for a decaying mode which becomes negligible well before horizon crossing. In the Newtonian gauge, one can thus take  $\Phi = 0$  or equivalently its source  $\delta_T^T \rho_T + \rho_s = 0$  as the initial condition.

## 2. Stress Structure

Causality constrains the possible forms which the stress perturbations can take. We generically expect white noise perturbations except in cases where conservation laws forbid their generation. In the latter case, stress fluctuations outside the horizon can fall off much steeper than white noise.

Let us first examine the case of a scalar field since it is relevant to cosmological defect models. Generically, the dynamics of a scalar field  $\phi$ , is governed by its Lagrangian  $\mathcal{L}(\phi, \dot{\phi})$ . The stress-energy tensor of the scalar field is

$$T_{\mu\nu} = \partial_\mu \phi \partial_\nu \phi - g_{\mu\nu} \mathcal{L}. \quad (\text{B10})$$

Thus, if we decompose its stresses, only the isotropic stress or “pressure,”

$$p_s = \frac{T_{ii}}{3}, \quad (\text{B11})$$

depends on both  $\dot{\phi}$  and  $\vec{\nabla}\phi$ , while the anisotropic stresses depend only on  $\vec{\nabla}\phi$ .

The causality constraint can be expressed as a condition on the auto-correlation function of  $\phi$ :

$$\langle \phi(\vec{r}, \tau) \phi(0, \tau) \rangle = 0 \quad \text{for} \quad r > \tau \quad (\text{B12})$$

where  $r$  is co-moving distance. If we expand  $\phi(\vec{r}, \tau)$  in terms of harmonic functions, this constraint implies that  $\phi(\vec{k}, \tau) \propto k^0$  for  $k\tau \ll 1$ :  $\phi$  behaves as “white noise” outside the horizon. The causality constraint also limits the spatial behavior of the derivatives of  $\phi$ :  $\dot{\phi}(\vec{k}, \tau)$  must scale as  $k^0$  or as some positive power of  $k$  to avoid producing superhorizon fluctuations and  $\vec{\nabla}\phi(\vec{k}, \tau) = i\vec{k}\phi(\vec{k}, \tau)$  must scale as  $k^1$  due to the constraint on the behavior of  $\phi$ . Thus  $T_{00}$  and the isotropic stress for the scalar field scales as white noise to lowest order, whereas anisotropic stress scales at  $k^2$  outside the horizon.

Just as energy-momentum conservation limits the form of the density fluctuation, additional symmetries can constrain the superhorizon scale behavior of the stress tensor. For example in electromagnetism, charge conservation

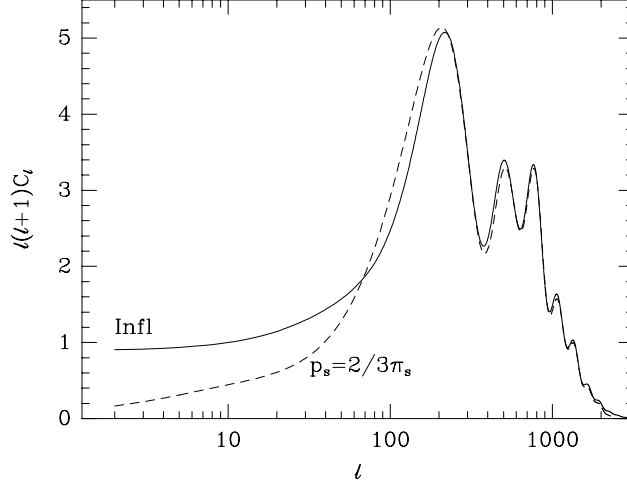


FIG. 5. Isocurvature model that mimics inflation. By choosing the stress-energy tensor of the seed to reverse the sign of gravity the general arguments of the main text are evaded. The anisotropy spectrum was calculated by a full Boltzmann calculation of the model of Eq. (C2) with  $A = 1$ ,  $B_1 = 1$ ,  $B_2 = 0.5$  with cosmological parameters  $\Omega_0 = 1$ ,  $h = 0.5$ ,  $\Omega_b h^2 = 0.0125$ .

restricts the spatial stresses produced by electromagnetism so that the large scale behavior of the fields implies that all of the stresses scale as  $k^2$  for small  $k$ . Charge conservation implies that causal processes can not create super-horizon correlations in charge or current density, nor can local monopoles be created. Summing random electric (or magnetic) dipoles leads to an electromagnetic field whose strength declines as  $1/L \sim k$  on superhorizon scales. Since the electromagnetic stress tensor,

$$T_{ij} = \frac{1}{4\pi} \left[ \frac{1}{2}(E^2 + B^2)\gamma_{ij} - E_i E_j - B_i B_j \right] \quad (\text{B13})$$

is quadratic in the field strengths, this small  $k$  behavior of  $E$  and  $B$  implies that both the isotropic and anisotropic stresses scale as  $k^2$  for small  $k$ . In magnetohydrodynamics, the isotropic component gives the magnetic pressure whereas the anisotropic part gives the  $\vec{J} \times \vec{B}$  force in the Euler equation. The Newtonian version of these calculations can be found in [34]. In this type of model, the specific signature in the CMB from white noise pressure contributions of §III B is replaced by the more general properties discussed in §III C.

### APPENDIX C: MIMICKING INFLATION

As discussed in §IIID, the ability of anisotropic stress to reverse the sign of gravity opens up the possibility of a loophole to the arguments behind the distinguishability of inflation from isocurvature models. For this to occur by the action of seed sources, the isotropic and anisotropic stresses must be exactly balanced so as to create no density perturbations from dynamical effects, yet still allow the anisotropic stress to generate gravitational potential perturbations. More specifically, we require  $\pi_s = 3p_s/2$  during the epoch when the acoustic oscillations form and for the scales on which they are observable. The  $(p_s, \pi_s)$  basis employed in the main text is not well suited to discuss this case since the isotropic and anisotropic stresses are assumed to be independent sources. Although that basis is natural for work on causal constraints, we must now search for an alternate representation to explicitly build a counterexample. We show here that properties of the model introduced by Turok [9] are a direct consequence of enforcing these rather special requirements.

There are four functions  $\rho_s$ ,  $p_s$ ,  $v_s$  and  $\pi_s$  that define the stress-energy tensor of the seed source and two constraint equations from energy-momentum conservation [see Eqs. (A4) and (A11)]

$$\begin{aligned} \frac{d}{d\tau} a^2 \rho_s + \frac{\dot{a}}{a} a^2 (\rho_s + 3p_s) &= -ka^2 v_s, \\ \frac{d}{d\tau} a^2 v_s + 2\frac{\dot{a}}{a} a^2 v_s &= ka^2 p_s - \frac{2}{3} ka^2 \pi_s, \end{aligned} \quad (\text{C1})$$

where we assume  $K/k^2 \rightarrow 0$ . This leaves two free functions that may be specified. Since  $p_s$  and  $\pi_s$  have different superhorizon scale behavior it is not possible to apply the desired constraint  $\pi_s = 3p_s/2$  directly. One way to enforce it is to require  $a^2 v_s \rightarrow 0$  for  $k\tau \gg 1$ . Momentum conservation also implies that  $a^2 v_s$  scales as  $k$  for  $k\tau \ll 1$ . The remaining condition can be taken as a causal constraint on  $\rho_s + 3p_s$ . Note that this choice directly specifies both of the synchronous gauge gravitational sources [see Eq. (A13)b,c].

Causality is enforced in the manner of §II C by requiring [6,9]

$$\begin{aligned} 4\pi G a^2(\rho_s + 3p_s) &= C_1 \tau^{-1/2} \frac{\sin(Ak\tau)}{(Ak\tau)}, \\ 4\pi G a^2 v_s &= C_2 \tau^{-1/2} \frac{6}{B_2^2 - B_1^2} \frac{1}{k\tau} \left[ \frac{\sin(B_1 k\tau)}{(B_1 k\tau)} - \frac{\sin(B_2 k\tau)}{(B_2 k\tau)} \right]. \end{aligned} \quad (C2)$$

For computational convenience, we relax the assumption of pure scaling in  $\rho_s + 3p_s$  at the matter-radiation transition, defining

$$C_1 = (\tau \dot{a}/a)^{-1}, \quad (C3)$$

which requires  $C_2$  to take the form,

$$C_2 = -\frac{2}{3} \frac{1}{1 + 4\tau \dot{a}/a}. \quad (C4)$$

Thus  $C_1$  and  $C_2$  interpolate between constants in the radiation and matter dominated epochs. An examination of Eq. (C1) shows that for  $k\tau \gg 1$  the stress-energy components take the form

$$a^2 \rho_s = -3a^2 p_s = -2a^2 \pi_s = \text{constant}, \quad a^2 v_s = 0 \quad (C5)$$

for *all*  $A, B_1, B_2$  as desired. The additional parameters merely determine at what point the model takes on this special form for the stress-energy tensor. Since  $\rho_s + 2\pi_s$  is the source of gravitational potential fluctuations of the seed  $\Psi_s$ , this implies that at late times

$$\Phi_s = \text{constant}, \quad \Psi_s = 0, \quad (C6)$$

and thus overdensities of the seed provide no gravitational attraction for the other matter components in the universe. It is important that  $\Phi_s$  and hence  $a^2 \rho_s$  are constant in order to remove metric “stretching” effects of the source as well as infall. Again this illustrates the very special nature of Eq. (C5): not only must there exist a relation between the stresses but also some components of  $T_{\mu\nu}$  must be *constant* while others must be *zero*. We comment on the stability of this situation below.

By breaking the relation between overdensities (or more strictly speaking curvature fluctuations) and potential fluctuations the door for mimicking inflation has been opened. One still needs to actually *reverse* the sign of gravity such that matter tends to fall out of overdense regions of the seed. This is readily achieved if an additional component such as cold dark matter (CDM) exists in the universe. Causality requires that this additional component have density fluctuations anticorrelated with the seed at horizon crossing. Since density fluctuations in this component create gravitational potential wells whereas those in the seed do not, the net result is that underdense regions of the seed correspond to gravitational potential wells. The fundamental criterion for the existence of a counterexample has now been met (see §III D). Furthermore, since these potential wells arise from CDM fluctuations and both the infall and “stretching” gravitational effects of the source are absent, they are constant in the matter-dominated epoch which results in a baryon-drag signal of alternating peaks that can closely mimic the standard-CDM inflationary prediction. We show an explicit calculation of such a model with  $A = 1$ ,  $B_1 = 1$ , and  $B_2 = 0.5$  in Fig. 5. The initial conditions are established in this synchronous gauge calculation to eliminate the components of the stress-energy pseudo-tensor by detailed balance of the seed and fluid components<sup>3</sup>.

Finally let us briefly discuss the implications of constraints of the form Eq. (C2) to support the claim that it is the special form of the stress-energy tensor in Eq. (C5) rather than some more general causal property that permits

---

<sup>3</sup>Specifically we take  $\dot{h} = (12/7)\sqrt{\tau_i}$ ,  $\delta_\gamma = \delta_\nu = -(4/9)\tau_i \dot{h}$ ,  $\delta_b = \delta_c = (3/4)\delta_\gamma$  and all other components zero. Formally the fluid velocities do not vanish, but we found that setting them to zero initially gave the same answers as including the compensation.

this counterexample. For example, in the synchronous gauge it might seem that fixing  $\rho_s + 3p_s$  *alone* is sufficient to determine the behavior of CMB fluctuations [6]. In synchronous gauge, the metric perturbation is specified by two functions,  $h$  and  $\eta$  [see Eq. (A7)]. The important point to note about the metric evolution equations (A13) is that  $h$ , but not  $\eta$ , is only dependent on the evolution of  $\rho + 3p$  type sources. Likewise the conservation equations (A8) and (A9) imply that before last scattering, the photon evolution is driven only by  $h$ . Thus the synchronous temperature perturbation at last scattering is purely determined by the assumption for  $\rho_s + 3p_s$ . This does *not* however imply that the structure of the observed anisotropy is so determined. To obtain the observed anisotropy, one must free-stream the radiation from the last-scattering surface to the present. After last scattering, the gravitational redshift from  $\eta$  which is dependent on the form of  $v_s$  generates photon quadrupole fluctuations [see e.g. [31] Eq. (63)]. This is in fact obvious from the Newtonian treatment which mixes  $\rho_s$ ,  $v_s$  and  $\pi_s$  in the gravitational source for acoustic oscillations in the effective temperature [see Eq. (17)]. Since gauge choice does not affect *physical observables*, the two must predict the same anisotropy for a given source model: they just choose to divide it into fluid temperature and gravitational redshift in different manners. Thus one cannot simply use the fluid temperature in synchronous gauge to make arguments about the corresponding temperature in the Newtonian gauge without fully specifying the model.

Now let us consider whether any other choice besides the asymptotic form of Eq. (C5) is possible for such seed contributions. Let us rewrite the conservation equation Eq. (C1) as

$$\left[ \frac{d^2}{d\tau^2} + 2 \left( \frac{\dot{a}}{a} \right) \frac{d}{d\tau} - \frac{1}{3} k^2 \right] 4\pi G a^2 \rho_s = - \left[ \frac{d}{d\tau} \left( \frac{\dot{a}}{a} \right) + 2 \left( \frac{\dot{a}}{a} \right)^2 + \frac{1}{3} k^2 \right] 4\pi G a^2 (\rho_s + 3p_s) + \frac{8}{3} \pi G a^2 k^2 \pi_s. \quad (C7)$$

If we also require  $a^2(\rho_s + 3p_s) \rightarrow 0$  as in Eq. (C2), then this equation is dynamically unstable and requires  $a^2 \rho_s$  to diverge unless  $\rho_s = -3p_s = -2\pi_s$ . Thus the only model that can be constructed out of the  $\rho_s + 3p_s$  form assumed in Eq. (C2), or indeed any form which implies  $|1 + 3p_s/\rho_s| \ll 1$  at late times, satisfies Eq. (C5). Such models *must* have the novel property of anisotropic stress fluctuations cancelling the gravitational attraction of matter to the seed overdensities. Of course, this relation need only hold for scales upon which acoustic peaks are visible in the CMB.

In summary, the counterexample of Turok [9] reconstructed here relies on very special properties of a specific stress-energy tensor and not on general properties of causally generated fluctuations.

- 
- [1] W. Hu & M. White, *Astrophys. J.* (in press, astro-ph/9602019); *ibid.*, *Phys. Rev. Lett* (in press, astro-ph/9602020).
  - [2] J.E. Lidsey, et al., *Rev. Mod. Phys.* (in press, astro-ph/9508078).
  - [3] R.G. Crittenden & N.G. Turok, *Phys. Rev. Lett* **75**, 2642 (1995) [astro-ph/9505120].
  - [4] J. Magueijo, A. Albrecht, D. Coulson & P. Ferreira, *Phys. Rev. Lett.* **76**, 2617 (1996) [astro-ph/9511042].
  - [5] R. Durrer, A. Gangui, & M. Sakellariadou, *Phys. Rev. Lett.* **76**, 579 (1996) [astro-ph/9507035].
  - [6] N. Turok, *Phys. Rev. D.* (in press, astro-ph/9604172).
  - [7] J.M. Bardeen, *Phys. Rev. D* **22**, 1882 (1980).
  - [8] H. Kodama & M. Sasaki, *Prog. Theor. Phys.* **78**, 1 (1984).
  - [9] N.G. Turok, DAMPT preprint, astro-ph/9607109.
  - [10] W. Hu & N. Sugiyama, *Phys. Rev. D* **51**, 2599 (1995) [astro-ph/9411008].
  - [11] Ya. B. Zel'dovich, *Adv. Astron. Astrophys.* **3**, 241 (1965).
  - [12] P.J.E. Peebles, *Astron. & Astrophys.* **32**, 391 (1974).
  - [13] B. Carr & J. Silk, *Astrophys. J.*, **268**, 1 (1983).
  - [14] J. Robinson, & B. Wandelt, *Phys. Rev. D* **53**, 618 (1996) [astro-ph/9507043].
  - [15] L.D. Landau & E.M. Lifshitz, *Fluid Mechanics*, (Pergamon Press, New York 1989).
  - [16] S. Veeraraghavan & A. Stebbins, *Astrophys. J.* **365**, 37 (1990).
  - [17] U.L. Pen, D.N. Spergel, & N. Turok, *Phys. Rev. D* **49**, 692 (1994).
  - [18] L. Abbott & J. Traschen, *Astrophys. J.* **302**, 39 (1986).
  - [19] P.J.E. Peebles, *Large Scale Structure of the Universe* (Princeton University Press, Princeton 1980).
  - [20] S. Weinberg, *Gravitation and Cosmology*, (Wiley, New York 1972) §11.
  - [21] J.M. Bardeen, P.J. Steinhardt, & M.S. Turner, *Phys. Rev. D* **28**, 679 (1983).
  - [22] D.H. Lyth, *Phys. Rev. D* **31**, 1792 (1985).
  - [23] T.W.B. Kibble, *J. Phys.* **A9**, 1387 (1976).
  - [24] A. Vilenkin and P. Shellard, *Cosmic Strings and Other Topological Defects* (Cambridge University Press, Cambridge 1994).
  - [25] M. Hindmarsh & T.W. Kibble, *Reports on Progress in Physics* **58**, 477 (1995).

- [26] N.G. Turok & D.N. Spergel, Phys. Rev. Lett. **66**, 3093 (1991).
- [27] J.A.N. Filipe & A.J. Bray, Phys. Rev. E**50**, 2523 (1994).
- [28] R.K. Sachs & A.M. Wolfe, Astrophys. J. **147**, 73 (1967).
- [29] C.L. Bennett, et al., Astrophys. J. Lett. **464**, L1 (1996) [astro-ph/9601067].
- [30] W. Hu, D. Scott, N. Sugiyama, & M. White, Phys. Rev. D**52**, 5498 (1995) [astro-ph/9505043].
- [31] C.-P. Ma & E. Bertschinger, Astrophys. J. **455**, 7 (1995) [astro-ph/9506072].
- [32] R. Durrer, Phys. Rev. D**42**, 2533 (1990).
- [33] M. White & D. Scott, Astrophys. J. **459**, 415 (1996) [astro-ph/9508157].
- [34] I. Wasserman, Astrophys. J. **224**, 337 (1982).

whu@sns.ias.edu

<http://www.sns.ias.edu/~whu>

dns@astro.princeton.edu

<http://www.astro.princeton.edu/~dns>

white@rigoletto.uchicago.edu

<http://www-astro-theory.fnal.gov/Personal/mwhite/welcome.html>